Journal of Nuclear Materials

Manufacturing Oxide Dispersion Strengthened (ODS) Steel Plate via Cold Spray and Friction Stir Processing

--Manuscript Draft--

Manuscript Number:	
Article Type:	VSI: ICFRM-21
Section/Category:	Structural materials
Keywords:	ODS Steels; GARS; Cold Spray; Friction Stir Processing; Manufacturing
Corresponding Author:	Dalong Zhang, PhD Pacific Northwest National Laboratory Richland, WA UNITED STATES
First Author:	Dalong Zhang, PhD
Order of Authors:	Dalong Zhang, PhD
	Xiang Wang, PhD
	Jens T Darsell, PhD
	Kenneth A Ross
	Xiaolong Ma, PhD
	Jia Liu, PhD
	Tingkun Liu, PhD
	Ramprashad Prabhakaran
	Lan Li, PhD
	Iver E Anderson, PhD
	Wahyu Setyawan, PhD
Abstract:	Oxide dispersion strengthened (ODS) steels, traditionally fabricated by ball milling and conventional powder metallurgy techniques, pose challenges in terms of scalability, and involve intricate processing steps such as rolling and thermal treatment to achieve plate or sheet formation. Here, we present a novel processing route that combines cold spray (CS) with friction stir processing (FSP) to manufacture ODS steel plate directly from gas atomization reaction synthesis (GARS)-prepared powder without rolling. Microstructural and mechanical characterizations were performed to assess the quality and properties of the resulting ODS steel plate. Our findings demonstrate that the slightly porous CS deposited layer was fully consolidated after FSP, yielding a dense ODS steel plate that exhibited a favorable tradeoff between strength and ductility upon extraction from the substrate. Furthermore, through microstructural analysis, we revealed the presence of an appreciable density (~1022/m3) of nano-sized oxide particles, with the majority being smaller than 5 nm via the combined CS + FSP fabrication route. This work serves as a first proof-of-concept demonstration of the manufacturing approach described herein, offering a promising alternative to the conventional methods for producing ODS steel plates.
Suggested Reviewers:	Michael Rieth, PhD Head of Department Metallic Materials, Karlsruhe Institute of Technology michael.rieth@kit.edu His leadership in ODS steel plate fabrication
	Yann de Carlan, PhD French Alternative Energies and Atomic Energy Commission Saclay Center yann.decarlan@cea.fr His expertise in ODS steel development and fundamental understanding.

Powered by Editorial Manager® and ProduXion Manager® from Aries Systems Corporation

Cover Letter

902 Battelle Boulevard
P.O. Box 999, MSIN K2-03
Richland, WA 99352
(509) 375-2575
dalong.zhang@pnnl.gov
www.pnnl.gov

June 28, 2023

Dear editor,

Please check the manuscript entitled "***Alternative fabrication route of ODS steel plate with cold spray and friction stir processing***" for your consideration on publication in ***Journal of Nuclear Materials*.**

Our work proposed a promising strategy to fabricate oxide dispersion-strengthened (ODS) steel plates by combining cold spraying (CS) and friction stir processing (FSP) without conventional ball milling and hot rolling. An appreciable density (~10^{22}/m3) of nano-sized oxide particles with an average diameter smaller than 5 nm were obtained in as-fabricated ODS steel plate after the combined CS + FSP fabrication route. This group of authors appreciate the opportunity to submit our original work to the JNM Special Issue for ICFRM-21. We believe the results from this first-of-its-kind work will benefit the broad research community in understanding the effects and benefits of severe plastic deformation-based methods as applied to nuclear and fusion materials (ODS steel in this case).

Thank you for time and consideration concerning this manuscript.

Sincerely,

Dalong Zhang, Ph.D.
(509) 375-2575
dalong.zhang@pnnl.gov

Highlights

- A novel approach combining cold spray deposition and friction stir processing was employed to fabricate the oxide dispersion strengthened (ODS) steel plate.
- The as-fabricated ODS steel plate showcased a remarkably uniform microstructure.
- High-density nano-sized oxide particles were formed in the newly fabricated ODS steel.

Graphical Abstract

Click here to access/download;Graphical Abstract;Graphical Abstract.jpg

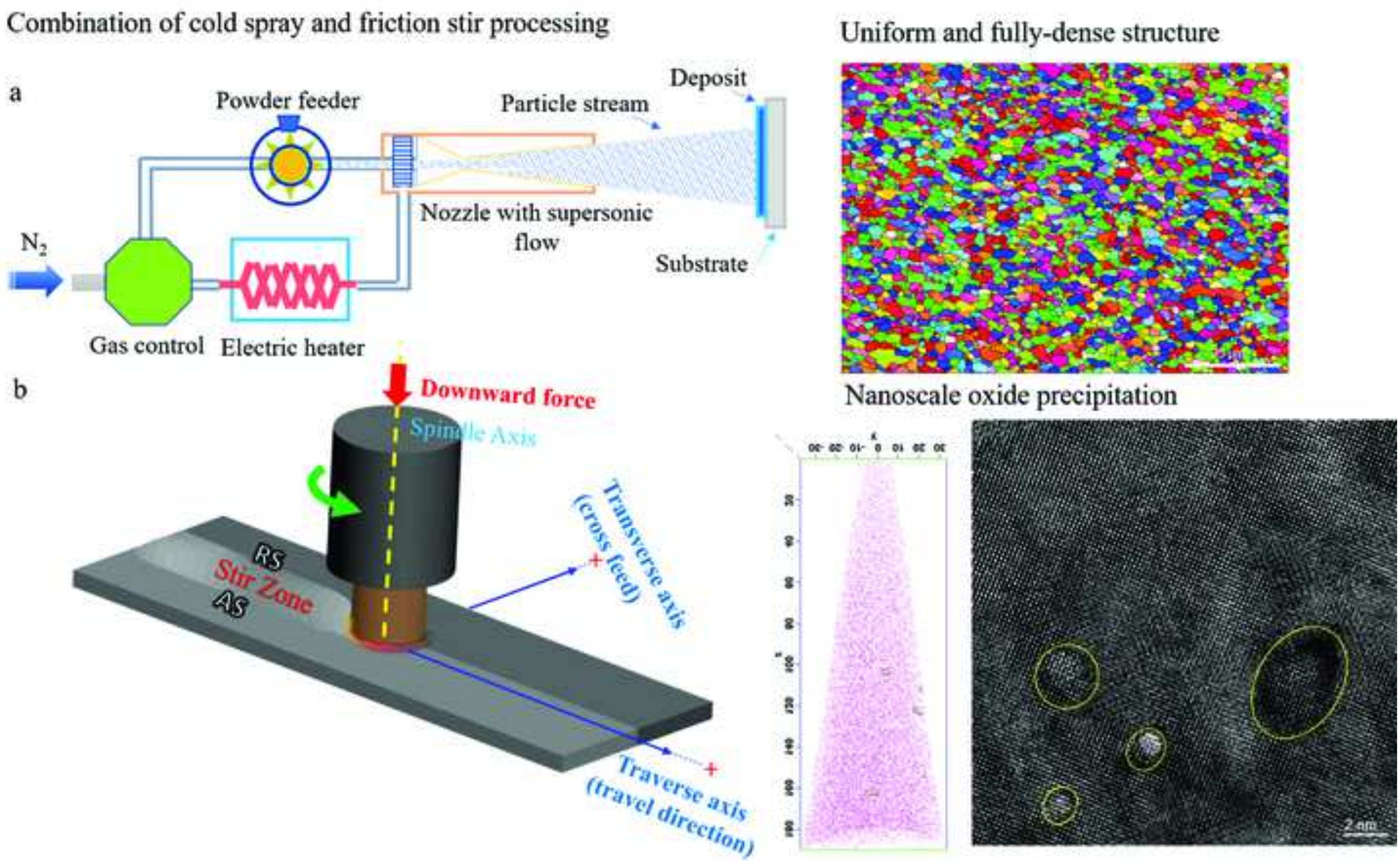

Manuscript File
Click here to view linked References

Manufacturing Oxide Dispersion Strengthened (ODS) Steel Plate via Cold Spray and Friction Stir Processing

Xiang Wang[a], Dalong Zhang[a]*, Jens T. Darsell[a], Kenneth A. Ross[a], Xiaolong Ma[a], Jia Liu[a], Tingkun Liu[a], Ramprashad Prabhakaran[a], Lan Li[a], Iver E. Anderson[b], Wahyu Setyawan[a]

[a] Pacific Northwest National Laboratory, Richland, WA 99352, USA

[b] Ames National Laboratory, Ames, IA 50011, USA

*Corresponding author. Email address: dalong.zhang@pnnl.gov (D. Zhang).

Highlights

- A novel approach combining cold spray deposition and friction stir processing was employed to fabricate the oxide dispersion strengthened (ODS) steel plate.
- The as-fabricated ODS steel plate showcased a remarkably uniform microstructure.
- High-density nano-sized oxide particles were formed in the newly fabricated ODS steel.

Graphical Abstract

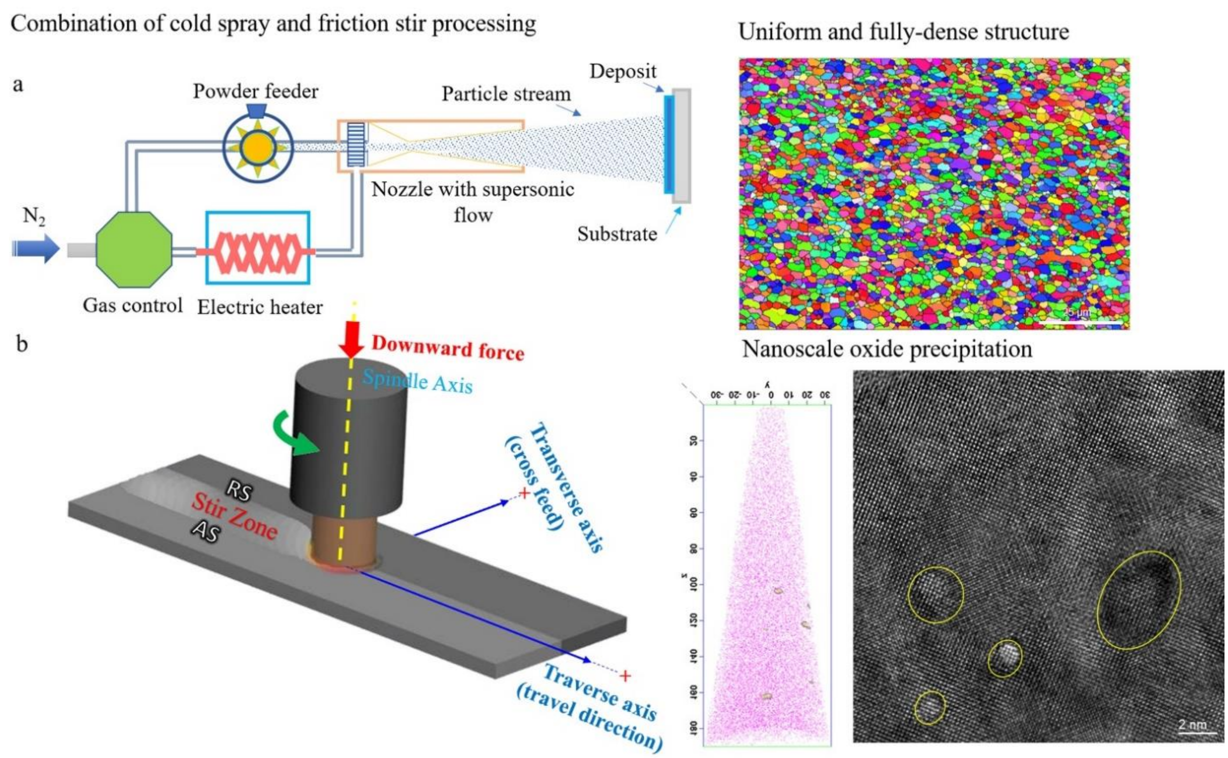

Abstract

Oxide dispersion strengthened (ODS) steels, traditionally fabricated by ball milling and conventional powder metallurgy techniques, pose challenges in terms of scalability, and involve intricate processing steps such as rolling and thermal treatment to achieve plate or sheet formation. Here, we present a novel processing route that combines cold spray (CS) with friction stir processing (FSP) to manufacture ODS steel plate directly from gas atomization reaction synthesis (GARS)-prepared powder without rolling. Microstructural and mechanical characterizations were performed to assess the quality and properties of the resulting ODS steel plate. Our findings demonstrate that the slightly porous CS deposited layer was fully consolidated after FSP, yielding a dense ODS steel plate that exhibited a favorable tradeoff between strength and ductility upon extraction from the substrate. Furthermore, through microstructural analysis, we revealed the presence of an appreciable density (~10^{22}/m^3) of nano-sized oxide particles, with the majority being smaller than 5 nm via the combined CS + FSP fabrication route. This work serves as a first proof-of-concept demonstration of the manufacturing approach described herein, offering a promising alternative to the conventional methods for producing ODS steel plates.

Keywords: ODS Steels; GARS; Cold Spray; Friction Stir Processing; Manufacturing

1. Introduction

Oxide dispersion strengthened (ODS) steels, as promising structural materials for future fusion power plants, are generally fabricated by a powder metallurgy technique termed mechanical alloying that is based on high-energy ball milling [1, 2]. Extremely high plastic strain imparted on the particulate feedstocks by ball milling results in the formation of fine and dispersed oxide particles forming in the ferritic steel matrix after consolidation and heat treatment steps [3, 4]. However, ball-milling-based techniques are challenging as a basis for scale-up and for reliable, cost-effective fabrication of ODS steels. Furthermore, billets prepared by ball milling and subsequent hot isotropic pressing/extrusion necessitate additional processing procedures such as hot rolling for plate forming [5-8]. Unfortunately, these additional steps can lead to the alignment of oxide particles as stringers [9] and the development of undesirable microstructural texture [10-12], resulting in property deterioration and anisotropy in ODS steels. The multiple steps and complex procedures involved in these conventional ODS steel manufacturing approaches often lead to nonuniform microstructures, undependable ductility, and lower efficiency with excessive costs.

To overcome these challenges, the cold spray (CS) technique has emerged as a potential solution. CS utilizes pressurized gas to propel powders onto a substrate material [13]. It offers the capability to directly manufacture scale-up ODS product shapes from improved ODS precursor powders, particularly those produced by gas atomization reaction synthesis (GARS) [14-16]. For example, CS has been explored to manufacture fuel cladding tubes [14, 15] and 14YWT ODS steels [17]. The low heat input in CS deposition deters any thermally induced transformation of feedstock powders, especially dissolution of the protective oxide surface, and evaporative composition losses [15]. However, when using CS technique to fabricate ODS steels/alloys from powders with enhanced strength, incomplete consolidation may occur due to the incomplete (and highly directional) bonding between particles, which induces the brittle fracture of cold-sprayed ODS samples [17]. CS also tends to impart some plastic deformation to the existing particle microstructure but does not specifically homogenize a heterogeneous particle. Consequently, post-treatments are required to modify the rough surface and work-hardened microstructure of cold-sprayed coatings [16]. On the other hand, friction stir processing (FSP), a solid-state processing method using a rotating pin to create extreme plastic deformation and mixing, has been successfully deployed for various applications mainly to refine the microstructure in the near-surface zone of a deposited layer [18, 19]. For instance, Huang et al. utilized FSP to modify the microstructure of cold-sprayed coatings such as SiC/Al5056 composite coating [20], Cu-Zn alloy coating [21], and Ni-Ti coating [22]. FSP treatment facilitated the redistribution and refinement of reinforcement particles [20], as well as the grain refinement and the formation of new phases [21, 22] in the coating. The resulting modified microstructure after FSP contributed to the enhancement of hardness and friction/wear resistance of coatings [20, 22], and even demonstrated the ability to "heal" microcracks caused by stress corrosion cracking [23]. Therefore, the controllable plastic deformation during FSP holds the potential for further optimizing and homogenizing the microstructure in ODS steels.

In this study, we present a promising technique combining CS and FSP to fabricate ODS steel using powder prepared with GARS. Microstructural characterization including scanning electron microscopy (SEM) coupled with energy dispersive X-ray spectroscopy (EDS), high-resolution transmission electron microscopy (TEM), and atom probe tomography (APT) were applied to demonstrate the formation of dispersed nano-sized oxide particles and the uniformity in the as-fabricated (i.e., CS + FSP) ODS plate. The mechanical properties of the ODS plate were also investigated.

Experiments

2.1 Materials

Powders prepared through GARS, a process conducted at Ames National Laboratory, were used for the fabrication of ODS steel plate. The distinctive characteristic of GARS ODS steel powder (i.e., GARS powder) is its comprehensive composition that encompasses all the essential elements for the formation of nano-sized pyrochlore oxide particles. The powder contains Ti in solid solution, O both in supersaturated solid solution [24, 25] and within Cr-rich oxide shell at powder surface. Additionally, Y predominately exists as Fe-Y intermetallic precipitates while also could be incorporated into the oxide shell. A detailed procedure of GARS can be found in Ref. [26]. Figure 1 shows the microstructure of ODS steel powder. The composition, measured through inductively coupled plasma atomic emission spectrometry and by SEM-EDS and corroborated by APT data, confirms the following weight percentages: Fe-14Cr-3W-0.35Y-0.40Ti. SEM backscattered electron (BSE) image proves that the initial powder is 45-90 μm in size, (Figure 1a and b), with a cellular grain structure present within. Significant enrichment of yttrium (Y) element can be observed near the cell boundaries (Figure 1c-e), in the form of Fe-Y intermetallics, whereas a portion of Y also presents in the powder surface oxide layer [19, 27]. The synchrotron x-ray diffraction (XRD) pattern (Figure 1g) indicates that the powder is composed of α-Fe, Y_2Fe_{17}, and Y_2TiO_5 phases.

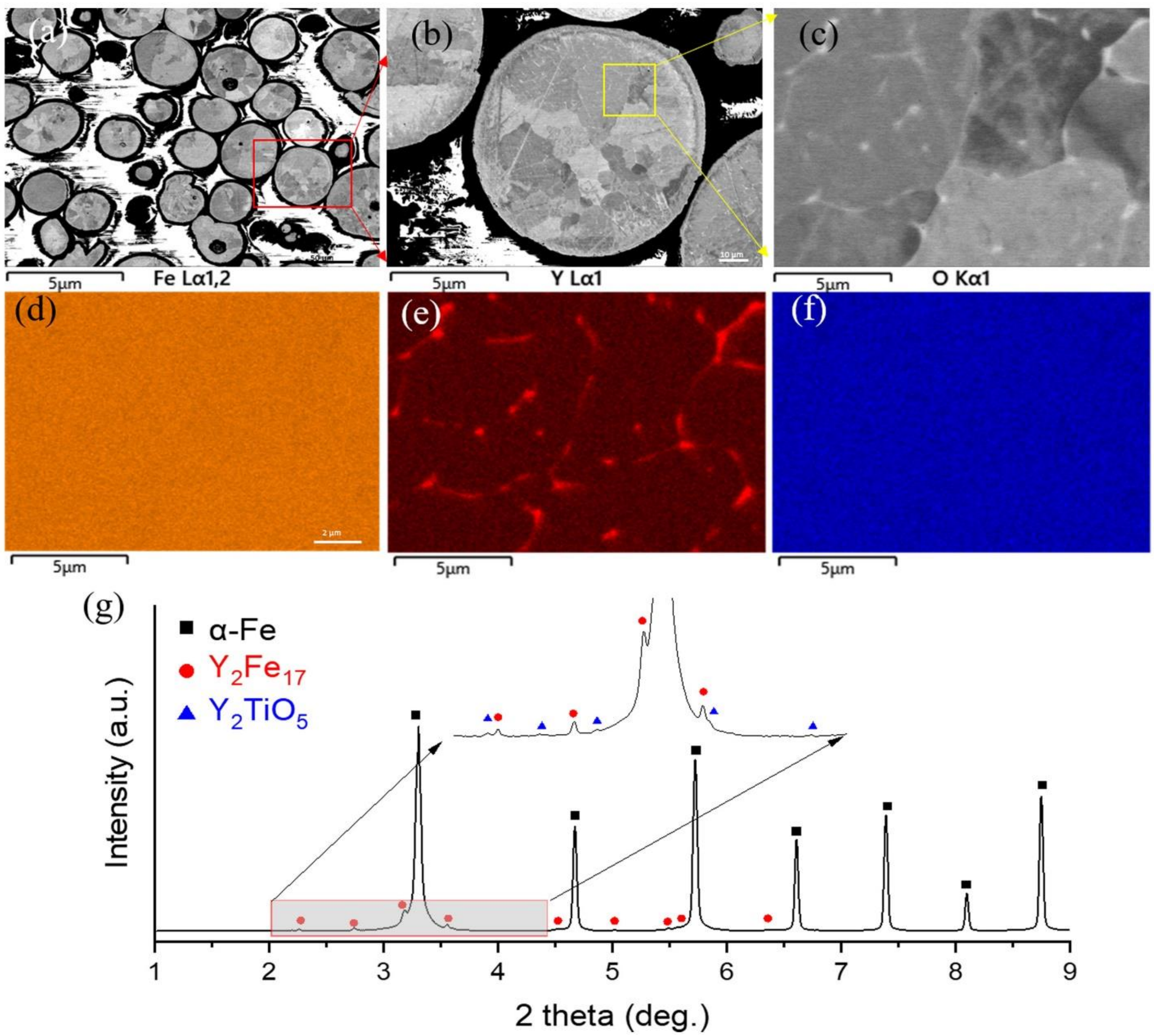

Figure 1. ODS steel powder prepared by GARS. (a) BSE image of ODS steel powder. (b) High-magnification BSE image of one selected powder. (c) High-magnification SEM image of the local region highlighted in b. (d, e, f) EDS mappings for Fe, Y, and O, respectively. (g) The synchrotron XRD pattern at a wavelength of 0.1173 Å. α-Fe, Y_2Fe_{17}, and Y_2TiO_5 are indexed.

2.2 Materials Processing

Figure 2 illustrates the revamped fabrication route of the ODS steel plate, achieved by combining CS with FSP using GARS powder. CS, depicted in Figure 2a, involves the solid-phase deposition of particles by accelerating them to supersonic velocities and allowing them to impact a substrate. In this study, the powder was propelled by pressurized supersonic gas flow from a nozzle to deposit on the P92 steel substrate in the high-pressure CS system [28]. CS was effectuated using a VRC Gen III CS system located at Pacific Northwest National Laboratory (PNNL). Helium carrier gas at ~4.1 MPa and 650°C was used for this work. The traverse speed, powder feeder rotation speed, standoff distance, and nozzle type were 200 mm/s, 8 RPM, 25 mm, and type 0058, respectively. To validate the applicability of empirically established CS parameters for steel powders to GARS powder with varying size ranges (45-75 μm and 75-90 μm), small trial coupons were first deposited. Following successful validation, a large area deposition (75 mm by 75 mm) was performed using a blend of the two size ranges mentioned above, resulting in a nominal thickness of 6 mm of ODS steel deposit on P92 steel substrate.

The ODS steel deposit was further densified and processed via FSP accomplished by employing a high stiffness and precision friction stir welding (FSW) machine (previously named Transformation Technologies Incorporated, now Bond Technologies) located at PNNL [29]. A schematic for the FSP process is shown in Figure 2b. FSP is a solid-phase process that involves spinning a tool and plunging it into the workpiece. Through frictional heating and material deformation, a plasticized region called the stir zone is formed beneath the tool shoulder. A Q-70 (70% Polycrystalline cubic boron nitride with 30% W-Re) CS4 (closed shoulder stepped spiral, 25.4 mm diameter convex shoulder and 6 mm pin with a stepped spiral on both pin and shoulder) tool purchased from Mazak MegaStir (Provo, UT) was used for FSP. During FSP, the tool traverses across the workpiece, creating a highly deformed stir zone. Temperatures generated during FSP typically range between 60% and 80% of the absolute melting temperature of the workpiece material. FSP was conducted herein in temperature control mode at 750°C, with a traverse rate of 25.4 mm/min and a force (Z-Force) of approximately 22 kN. The tool followed a raster pattern to ensure sufficient tool shoulder overlap for complete lateral and through-thickness processing of the plate. To further process the large area CS deposit with FSP, a proof-of-concept raster FSP run was designed using temperature control mode. Figure 2c displays the FSP tool position-temperature plot based on the actual data logged by the FSW machine. The gray dotted circles stand for the approximate profile of the tool area engaged with the material, while the black dotted arrows indicate the traverse directions of the tool. The raster started from the “zero position” of the machine, with the tool moving from left to right. Within the initial ~15 mm travel, the tool temperature ramped up to 770°C and then stabilized at the set point temperature of 750°C. Subsequently, with the stable temperature of 750°C as moderated by the rotational speed, the tool traversed further to the right by ~22 mm, followed by upward movement of ~8 mm, and finally to the left by ~37 mm before undergoing extraction sequence (not plotted). Taking the tool profile into consideration, this simple FSP raster run successfully processed a significant area of the large CS deposit, approximately 50 mm long and 25 mm wide. The purple dotted line represents the approximate location where a cross-section specimen was extracted using electrical discharge machining (EDM) for subsequent microstructure and hardness studies.

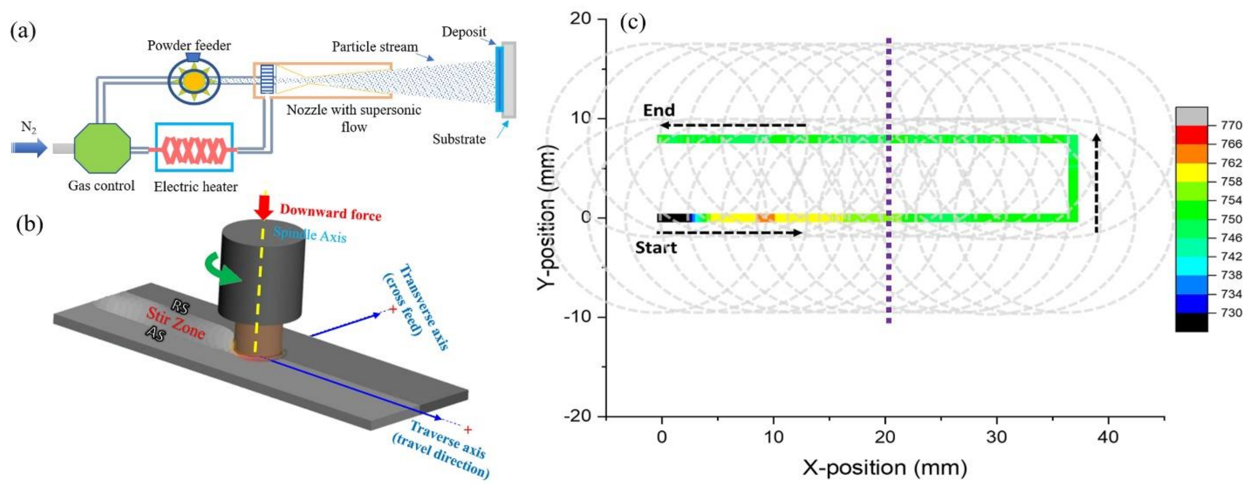

Figure 2. Schematic of the no-hot-rolling-needed process for ODS steels. (a) CS. (b) FSP. (c) The FSP tool position-temperature plot based on the actual data logged by the FSW machine.

2.3 Microstructural Characterization

ODS steel powder was analyzed using synchrotron XRD with the wavelength of 0.1173 Å at Beamline 11-ID-C of the Advanced Photon Source, Argonne National Laboratory. Two-dimensional diffraction pattern was analyzed using GSAS-II software [30]. The diffraction peak intensity of the primary phase was reduced by a threshold mask to highlight weak peaks of the secondary phases.

Metallographic cross-section samples obtained from fabricated (CS + FSP) ODS steel plate were prepared following the standard metallographic procedure, with colloidal silica vibratory polishing as the last step. Macro- and microstructures were examined using optical microscopy, followed by SEM-EDS analysis using a JSM-IT500 SEM equipped with dual 100 mm^2 Oxford EDS detectors. In addition, electron backscattered diffraction (EBSD) mapping was carried out on either a FEI (now Thermo Fisher Scientific) Helios 660 SEM equipped with an EDAX EBSD detector or a Helios 5 Hydra SEM implemented with an Oxford Symmetry EBSD detector at an accelerating voltage of 30kV.

TEM specimens were prepared via the focused-ion beam (FIB) technique (routine lift-out and thinning procedure) by employing a FEI Helios 660 SEM/FIB. TEM/scanning TEM (STEM) observations were performed on JEOL GrandARM 300CF AC-Scanning TEM, FEI Titan 80-300 Environmental Cs-corrected TEM, and Themis Z 30-300 Monochromated Aberration Corrected STEM.

APT specimens were prepared using FIB according to the standard lift-out procedure [31]. The analysis was conducted using a CAMECA LEAP4000 XHR system under ultraviolet laser-assisted mode, with the following conditions: pulse energy of 100 pJ, evaporation rate of 5 evaporation events per 1,000 pulses, pulse repetition rate of 200 KHz, and a base temperature of 40 K. The APT results were reconstructed using Interactive Visualization and Analysis Software (IVAS 3.8).

2.4 Mechanical Testing

Vickers microhardness testing was performed (500 gf and 12 s dwell time) on polished cross-section samples obtained from the ODS steel plate. Hundreds of indents (0.3 mm apart) were made across extended areas on polished samples to obtain a hardness profile. EDM was used to obtain subsize tensile specimens (SS-J2 type [32]) from CS + FSP ODS steel plate. The nominal gage width, gage thickness, and reduced length were 1.2 mm, 0.4 mm, and 5.0 mm, respectively. The total length and shoulder width of the specimen are 16 mm and 4 mm, respectively. The specimen gage width and thickness were measured using calipers before tensile testing. An Instron 8801 servo-hydraulic mechanical testing system was used for conducting tensile testing in displacement control mode. The displacement rate during tensile testing was constant at a crosshead speed of 0.03 mm/min, which can be converted to an estimated strain rate of 1E-4/s for SS-J2 specimens. Tensile testing was performed using shoulder-loaded grips at ambient temperature. The ASTM E8 Standard was used for tensile testing and data analysis [33]. The displacement was measured from the crosshead movement. Engineering stress-strain curves were generated by using the load-displacement data recorded during testing along with specimen dimensions. These curves were used to determine 0.2% offset yield strength, ultimate tensile strength, uniform elongation, and total elongation.

3 Results

3.1 Microstructure of the CS + FSP Fabricated ODS Steel Plate

To assess the feasibility of the CS deposition for manufacturing ODS steel plates, the microstructures of the CS layers were investigated using coupon-size (25 mm × 25 mm) P92 steel substrates. Two powder size ranges, 45-75 μm and 75-90 μm, were used from GARS powder. Cross-section optical microscopy images (Figure 3a and f) showed deposition layers of approximately 1.5 mm and 1.6 mm for the 45-75 μm (Figure 3a) and 75-90 μm (Figure 3f) powder, respectively, on the P92 steel substrate after CS deposition. The bonding between the deposition layer and substrate was imperfect, as evidenced by consecutive wave-like microcracks at the interface observed via SEM (Figure 3b and g). The deposition layer presented a heavily deformed structure indicated by the spindle-shaped grains, which was consistent with results reported in the literature for CS [14, 15, 28, 34]. EBSD mapping (Figure 3c and h) revealed the formation of submicron fine grains near the cracks/pores, resulting from the localized severe plastic deformation, adiabatic shear, and dynamic recrystallization during the high-velocity impact between powder particles [28]. Compared to the "shell" region of powder, grains in the powder interior experienced a relatively lower deformation with high residual stress after CS (Figure 3d and i). Hardness mapping confirmed the presence of an inhomogeneous distribution (Figure 3e and j), indicating the significant structure heterogeneity induced by CS. These results implied that the initial powder size did not result in a noticeable difference in the final microstructure after CS. Therefore, a mixture of powders from the two size ranges (45-75 μm and 75-90 μm) was used to prepare the ODS steel plate.

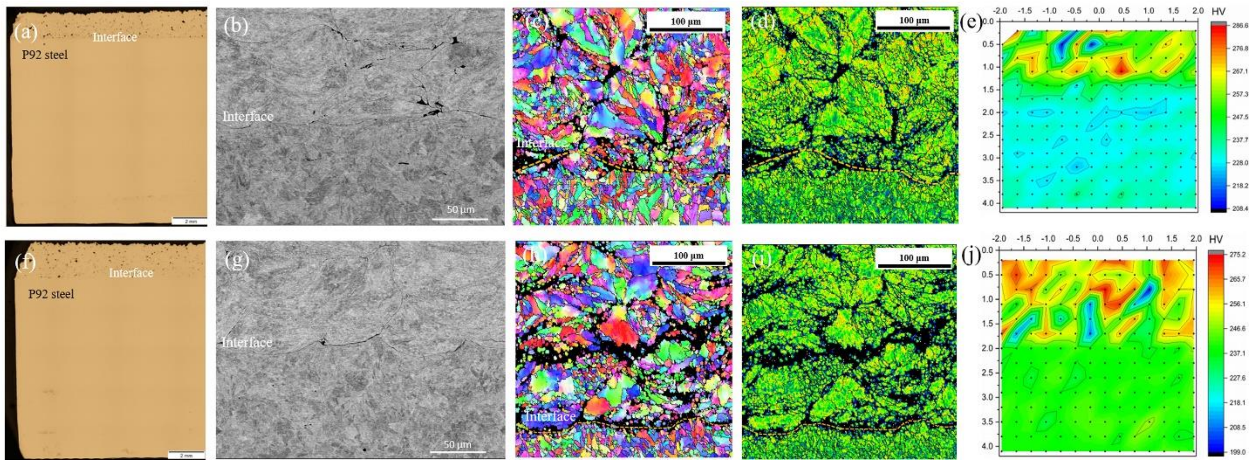

Figure 3. Examples of CS for powder of two sizes. (a) CS sample with 45–75 μm powder on the mild steel substrate. (b) Interface of the (a) sample. (c) EBSD mapping of the interface in the (a) sample. (d) Corresponding Kernel Average Misorientation mapping. (e) Vicker harness. (f-j) CS sample with 75–90 μm powder and its corresponding microstructure.

It is worth noting that the CS deposited layer still exhibited appreciable porosity and a nonuniform structure. To further densify and refine the ODS steel microstructure, FSP was performed on the large (75 mm by 75 mm) CS deposit. Given the thickness of the CS deposit (~6 mm), a 6 mm pin FSP tool was used. Subsequently, for ease of handling and preparation of specimens for characterization and mechanical testing, the top ~3 mm thickness of the CS + FSP plate was relieved from the substrate by EDM. Figure 4 illustrates the microstructures of the ODS plate processed by combined CS + FSP at 750°C. Two distinct zones were observed as a result of FSP treatment: the stir zone (directly under the tool pin) and the overlap zone (intersection between two separate FSP passes at the shoulder of the tool) (Figure 4a). The insert in Figure 4a is a side view of the SS-J2 tensile specimen schematic, indicating the size and approximate location of tensile specimens relative to the ~3 mm thick ODS steel plate relieved from the substrate. Namely, the tensile specimen intentionally contains both the overlap zone and the stir zones in the gauge, as an effort to evaluate the overall mechanical integrity of the plate. After FSP, grains within the stir zone were further refined to 1.7 μm average size, forming an equiaxed-grain microstructure (Figure 4b and c). The grain refinement after FSP is attributed to the applied plastic deformation and accompanying recrystallization during FSP [35]. Furthermore, the initial porous layer transformed into a densified structure without cracks or pores (Figure 4b and c). The densification effect is believed to be a result of the compression force and dynamic material flow provided by FSP. TEM characterization revealed the dispersion of nano-sized particles in the steel matrix, with a number density on the order of $10^{22}/m^3$, assuming a TEM specimen thickness of ~30 nm (Figure 4d and e). A high-resolution TEM image (Figure 4f) exhibited nano-sized particles below 5 nm, and a slightly larger particle (~15 nm) imaged in Figure 4g showed a clear Fast Fourier Transform (FFT) pattern matching the structure of Y_2TiO_5.

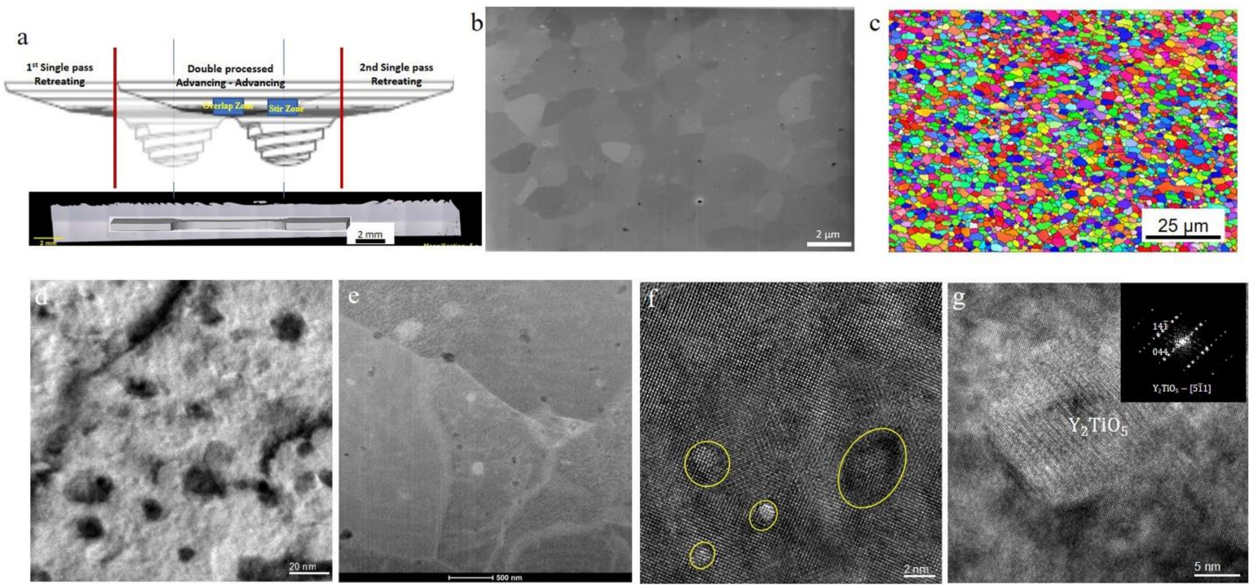

Figure 4. CS + FSP fabricated ODS steel plate based on GARS prepared powder. (a) Schematic of FSP at 750℃ for the preparation of ODS steel plate. Cross-section of ODS steel shown below, along with the side view of a schematic of the SS-2J tensile specimen indicating the size of the specimen relative to the plate, as well as the approximate location of the specimen in the plate. The top ~3 mm thickness of the CS + FSP plate was relieved from the substrate by EDM. (b) BSE image of the stir zone. (c) EBSD mapping of the stir zone. (d) Low-magnification TEM and (e) STEM images containing particles. (f) HRTEM image of nano-sized oxides as highlighted by circles. (g) HRTEM image of one Y_2TiO_5 particle. Fast Fourier Transform (FFT) pattern of the oxide particle inserted.

To investigate the microstructure uniformity after FSP, the overlap zone was also characterized (Figure 5). The average grain size within the overlap zone was ~2 μm (Figure 5a), indicating uniform refinement of the grain structure induced by FSP [36]. High density of dispersed particles was also observed within the overlap zone (Figure 5b). Another larger particle was imaged in Figure 5c, and its lattice parameter matches that of Y_2TiO_5.

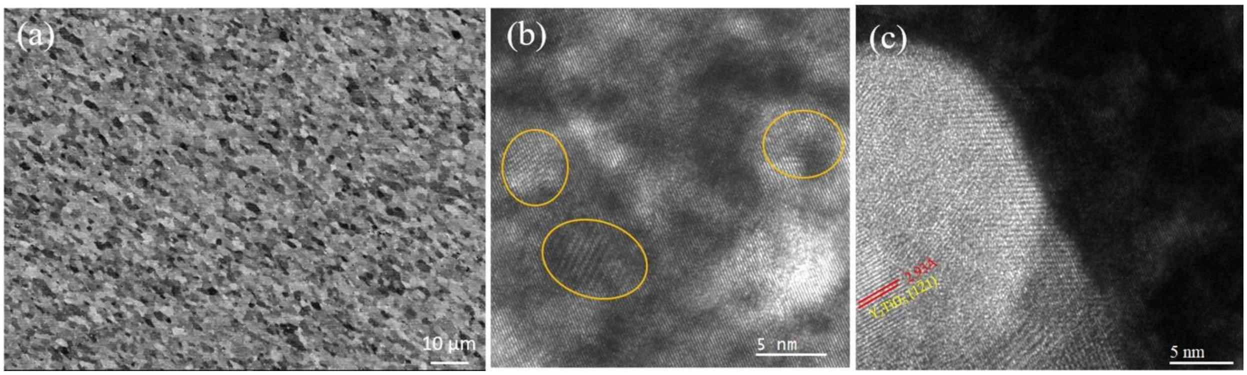

Figure 5. Microstructure of the overlap zone in the CS + FSP fabricated ODS steel plate. (a) Low magnification BSE image. (b) HRTEM image. Nano-sized oxide particles are circled. (c) HRTEM image of one large Y_2TiO_5 particle.

Preliminary APT characterization was carried out to investigate the spatial distribution and composition of the nano-sized particles within the stir zone and overlap zone (Figure 6). Note that isosurface of 0.7 at.% Y was used in Figure 6a and 6g to better visualize the clusters containing Y, O, and possibly Ti [37]; also, other alloying elements, i.e., Cr and W, are randomly distributed in the Fe-matrix, thus not shown here. As indicated by ion maps of O, YO, Y, Ti, TiO in Figure 6b–f, the nano-sized particles were Y-(Ti)-O oxide particles randomly dispersed in the matrix with a $1.6 \times 10^{22}/m^3$ number density, coinciding with TEM results in Figure 4. APT characterization within the overlap zone also showed similar results (Figure 6h–l). The severe plastic deformation applied by FSP effectively dispersed Y elements in the steel matrix [19, 38], compared to the original oxide shells and the cellular distribution of Fe-Y intermetallic phase in the GARS prepared powder. The supersaturated O (bulk concentration 0.086 ± 0.001 at % in Figure 6b and 0.301 ± 0.002 at % in Figure 6h) in the matrix [24, 25], along with a normal solid solution of Ti, offered the precondition for dispersed Y element to form fine Y-(Ti)-O particles under heating and deformation during FSP [19]. Further investigation is ongoing to explore the microstructure, the underlying formation mechanisms of oxide particles, and the effects of temperature.

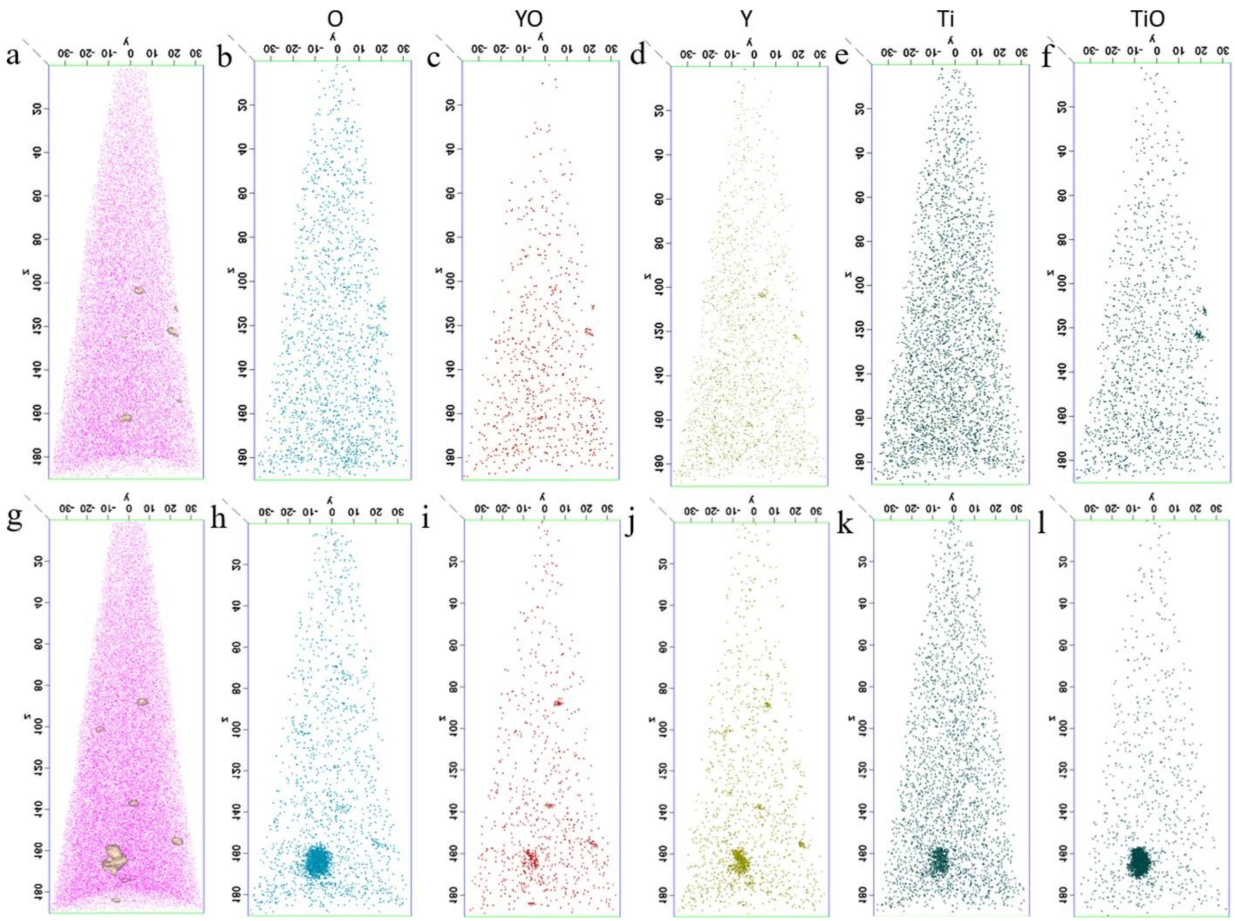

Figure 6. Dispersed nano-sized oxide particles in CS + FSP fabricated ODS steel plate. (a) Three-dimensional APT reconstruction of the specimen in the stir zone of ODS steel plate. Isosurface of 0.7 at.% Y is used to better visualize Y-containing clusters. (b–f) Corresponding interested ion maps extracted from APT in (a). (g) Three-dimensional APT reconstruction of the specimen in the overlap zone of ODS steel plate. (h–l) Corresponding interested ion maps extracted from APT in (g).

3.2 Mechanical Properties of the CS + FSP Fabricated ODS Steel Plate

Finally, hardness mapping showed the homogeneous distribution of hardness in the ODS steel plate fabricated by CS + FSP (Figure 7a–c), verifying the microstructural uniformity. The average Vickers hardness was 216 ± 15 HV. Note that at the bottom right corner of the plate, a small region of porous CS deposit can be seen, which is outside of the FSP process zones, and was intentionally preserved for future comparative study. The tensile properties (two specimens tested) were also evaluated by the quasi-static tensile test at room temperature, shown in Figure 7d. The initial nonlinear portion of the stress-strain curve was due to the compliance of the test frame and that between the SS-J2 specimen and the fixture. The average 0.2% offset yield strength and ultimate tensile strength are 540 MPa and 700 MPa, respectively. Even though the strength is lower compared to the 14YWT ODS steels processed by ball milling and hot extrusion (~1 GPa) [39-41], the ODS steel plate herein shows a good strength–ductility tradeoff, proved by the uniform elongation of 8.8% and total elongation of 20.8%.

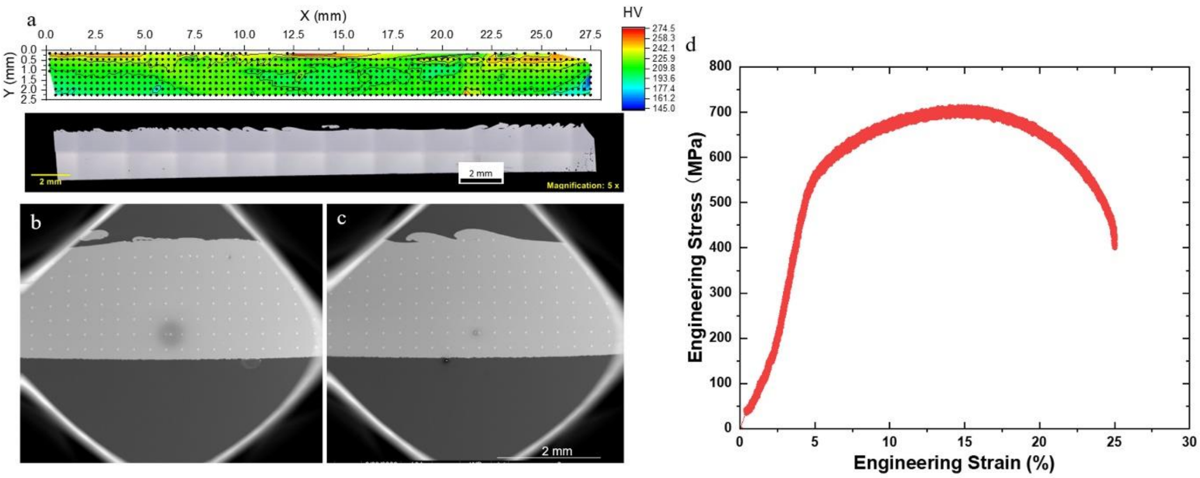

Figure 7. Mechanical properties of CS + FSP fabricated ODS steel plate. (a) Hardness mapping of the ODS steel plate. (b) SEM image of indents in the stir zone. (c) SEM image of indents in the overlap zone. (d) Engineering stress-strain curves of ODS steel plate.

4 Discussion

High-pressure CS systems typically operate at pressures ranging from ~2.1 to 6.9 MPa [42] and produce particle velocities ranging from 800 to 1,400 m/s [13]. The high velocity of the particles enables a high kinetic energy, leading to significant impact energy during the spraying process. This energy plastically deforms the material at the interface, resulting in dynamic recrystallization and the formation of a mechanical interlock and metallurgical bonding between the deposited material and the substrate (Figure 3). Metallurgical bonding at interparticle boundaries is also induced by severe plastic deformation and shear at the powder surface. Importantly, the CS process minimizes substrate heating, ensuring dimensional stability and avoiding detrimental thermal effects such as thermal stresses and dilution layer formation. This makes CS an attractive method for depositing GARS powder since its microstructure remains intact or slightly refined during the CS process, without being coarsened by high heat input or melting. FSP is the use of FSW setup for purposes other than joining, such as material property modification and repair. In the context of CS + FSP, FSP further refines and homogenizes the microstructure while eliminating residual cracks or pores left from the CS process (Figure 4). The controlled heat input in FSP plays a role like post-deposition heat treatment, allowing for microstructure optimization in the deposition layer. In certain material systems, such as austenitic stainless steels, FSP can even improve the mechanical properties and corrosion resistance when performed at sufficiently low temperature (e.g., 700–800°C) [29, 43]. FSP of deposited GARS powder has been proven to produce a fine-grained structure with increased refinement and distribution for oxide particles through additional plastic deformation and dynamic recrystallization [35]. Notably, a relatively low processing temperature in FSP (750°C) does not prompt observable coarsening of oxide particles and the detailed effect of processing temperature in FSP on the microstructure and properties of ODS steel plates is an ongoing study. The ability to process at elevated temperature and exemption of property deterioration in CS + FSP fabricated ODS steel plates is expected to extend the service life of FSP tools and improve their cost efficiency. The combination of CS with FSP not only eliminates the need for multistep processing steps such as milling, rolling, and annealing post-treatment in the manufacturing of ODS steels [1, 4], but also advances the CS manufacturing technology for practical applications [15, 16]. Meanwhile, additive manufacturing (AM) as a newly-developed approach is being explored to fabricate ODS steels [44, 45]. However, the high temperatures required in the printing process can easily induce nanoparticle aggregation and coarsening [44, 45]. The optimization of process parameters, powder compositions, and heat treatment conditions is an ongoing task in the AM fabrication process of ODS steels, along with the investigation of the underlying mechanisms responsible for the obtained microstructure. The CS + FSP approach, with its low-temperature processing route, offers additional flexibility for adjusting various processing parameters.

The favorable strength–ductility tradeoff achieved in CS + FSP fabricated ODS steel plate benefits from the synergistic effect of various mechanisms. In addition to the strengthening through grain refinement based on the Hall-Petch effect [46, 47], dispersed oxide particles also play a role in strengthening ODS steel plate. Fine oxide particles provide significant Orowan strengthening by effectively impeding the motion of dislocations [1, 48-50]. The supersaturated oxygen [24, 25] and W/Cr solutes in the steel matrix contribute to the solid solution strengthening. Considering the typical oxide particle density in ODS steels at ~$10^{23}/m^3$ [1], the observed lower strength in the CS + FSP fabricated ODS steel plate, compared to ODS steels processed through ball milling, may be attributed to the relatively larger grain size and lower oxide particle density

($\sim 10^{22}/m^3$) in the CS + FSP fabricated plate. This, along with the micron-sized grain structure, contrasts with the ultrafine-grained ODS steels produced by ball milling. However, the > 1 μm grain size in CS + FSP fabricated ODS steel reserve the capacity to accommodate plastic deformation [51], giving rise to excellent ductility. Further optimization of the ODS steel microstructure through subsequent thermal treatment and modification of the processing parameters can improve the mechanical properties of ODS steel fabricated by CS + FSP. Additionally, the ongoing development of new generations of GARS feedstock powders, incorporating varying Y, Ti, and O contents, as well as different morphologies of Fe-Y intermetallic phases and surface oxide layer thickness, holds promise for improving the density of nano-sized oxide particles in the ODS steel.

5 Conclusions

The integration of CS with FSP presents a novel approach for the fabrication of ODS steel plates using GARS prepared powder, eliminating the need for traditional processes such as ball milling and hot rolling. Our preliminary findings have demonstrated the effectiveness of the CS + FSP route in consolidating the powder and refining both the grain and oxide structures. This results in the formation of a uniform and fully dense microstructure, along with an appreciable density of nano-sized oxide particles ($\sim 10^{22}/m^3$). The proposed processing route offers several advantages over conventional methods, including the avoidance of laborious steps such as ball milling, canning, degassing, and hot/cold rolling. Moreover, the CS + FSP approach is highly scalable and not limited by dimensions, making it a promising pathway for the future fabrication of ODS steel plates. The successful implementation of this technique holds great potential in streamlining the manufacturing process and enabling the production of ODS steel plates on a larger scale.

CRediT Authorship Contribution Statement

Xiang Wang: Validation, Formal analysis, Investigation, Writing - Original Draft, Writing - Review & Editing, Visualization. **Dalong Zhang**: Conceptualization, Methodology, Formal analysis, Investigation, Writing - Original Draft, Writing – Review & Editing, Visualization, Supervision, Funding acquisition. **Jens Darsell**: Methodology, Investigation, Writing - Review & Editing. **Kenneth Ross**: Methodology, Investigation, Writing - Review & Editing. **Xiaolong Ma**: Formal analysis, Visualization. **Jia Liu**: Formal analysis, Visualization. **Tingkun Liu**: Formal analysis, Visualization. **Ramprashad Prabhakaran**: Validation, Formal Analysis. **Lan Li**:

Validation, Visualization. **Iver Anderson**: Resources, Writing - Review & Editing. **Wahyu Setyawan**: Resources, Supervision.

Declaration of Competing Interest

The authors declare no conflict of interest.

Acknowledgments

This research is funded by the U.S. Department of Energy Office of Fusion Energy Sciences under contract DE-AC05-76RL01830 (FWP 13784). We are grateful to cold spray technical support provided by Chris Smith, Daniel Graff, Gary Neuenschwander, and Eric Loeffler. We thank Anthony Guzman, Michael Blazon, and Angel Ortiz for metallography and hardness tests. We also thank Jacqueline Royer for gathering electron backscattered diffraction data. Pacific Northwest National Laboratory is operated by Battelle Memorial Institute for the United States Department of Energy under Contract DE-AC06-76RLO1830. Ames National Laboratory is operated by Iowa State University for the United States Department of Energy under Contract No. DE-AC02-07CH11358. This work was performed, in part, at the William R. Wiley Environmental Molecular Sciences Laboratory, a national scientific user facility sponsored by U.S. Department of Energy, Office of Biological and Environmental Research and located at PNNL.

Funding

This research is funded by the U.S. Department of Energy Office of Fusion Energy Sciences under contract DE-AC05-76RL01830.

Data Availability Statement

All data needed to evaluate the conclusions are present in the paper.

References

[1] G.R. Odette, N. Cunningham, T. Stan, M.E. Alam, Y. Carlan, Nano-Oxide Dispersion-Strengthened Steels, 2019, pp. 529-583.
[2] S. Ukai, S. Ohtsuka, T. Kaito, Y. De Carlan, J. Ribis, J. Malaplate, Oxide dispersion-strengthened/ferrite-martensite steels as core materials for generation IV nuclear reactors, Structural Materials for Generation IV Nuclear Reactors, Elsevier2017, pp. 357-414.
[3] J.S. Benjamin, Dispersion strengthened superalloys by mechanical alloying, Metallurgical transactions 1(10) (1970) 2943-2951.

[4] J. Wang, S. Liu, B. Xu, J. Zhang, M. Sun, D. Li, Research progress on preparation technology of oxide dispersion strengthened steel for nuclear energy, International Journal of Extreme Manufacturing 3(3) (2021) 032001.
[5] I. Kubena, B. Fournier, T. Kruml, Effect of microstructure on low cycle fatigue properties of ODS steels, Journal of Nuclear Materials 424(1) (2012) 101-108.
[6] D.T. Hoelzer, K.A. Unocic, M.A. Sokolov, T.S. Byun, Influence of processing on the microstructure and mechanical properties of 14YWT, Journal of Nuclear Materials 471 (2016) 251-265.
[7] I.-S. Kim, B.-Y. Choi, C.-Y. Kang, T. Okuda, P.J. Maziasz, K. Miyahara, Effect of Ti and W on the mechanical properties and microstructure of 12% Cr base mechanical-alloyed nano-sized ODS ferritic alloys, ISIJ international 43(10) (2003) 1640-1646.
[8] R. Lindau, A. Möslang, M. Rieth, M. Klimiankou, E. Materna-Morris, A. Alamo, A.-A. Tavassoli, C. Cayron, A.-M. Lancha, P. Fernandez, Present development status of EUROFER and ODS-EUROFER for application in blanket concepts, Fusion Engineering and design 75 (2005) 989-996.
[9] X. Mao, T.K. Kim, S.S. Kim, K.H. Oh, J. Jang, Thermal stability of oxide particles in 12Cr ODS steel, Journal of nuclear materials 428(1-3) (2012) 82-89.
[10] S. Ukai, M. Fujiwara, Perspective of ODS alloys application in nuclear environments, Journal of Nuclear Materials 307-311 (2002) 749-757.
[11] Z. Oksiuta, P. Hosemann, S.C. Vogel, N. Baluc, Microstructure examination of Fe–14Cr ODS ferritic steels produced through different processing routes, Journal of Nuclear Materials 451(1) (2014) 320-327.
[12] A. Das, H. Viehrig, F. Bergner, C. Heintze, E. Altstadt, J. Hoffmann, Effect of microstructural anisotropy on fracture toughness of hot rolled 13Cr ODS steel–The role of primary and secondary cracking, Journal of Nuclear Materials 491 (2017) 83-93.
[13] A. Moridi, S.M. Hassani-Gangaraj, M. Guagliano, M. Dao, Cold spray coating: review of material systems and future perspectives, Surface Engineering 30(6) (2014) 369-395.
[14] M. Lenling, H. Yeom, B. Maier, G. Johnson, T. Dabney, J. Graham, P. Hosemann, D. Hoelzer, S. Maloy, K. Sridharan, Manufacturing oxide dispersion-strengthened (ODS) steel fuel cladding tubes using the cold spray process, Jom 71(8) (2019) 2868-2873.
[15] B. Maier, M. Lenling, H. Yeom, G. Johnson, S. Maloy, K. Sridharan, A novel approach for manufacturing oxide dispersion strengthened (ODS) steel cladding tubes using cold spray technology, Nuclear Engineering and Technology 51(4) (2019) 1069-1074.
[16] H. Yeom, K. Sridharan, Cold spray technology in nuclear energy applications: A review of recent advances, Annals of Nuclear Energy 150 (2021) 107835.
[17] H. Yeom, D. Hoelzer, S. Maloy, K. Sridharan, Cold spray manufacturing of oxide-dispersion strengthened (ODS) steels using gas-atomized and ball-milled 14YWT powders, Journal of Nuclear Materials 574 (2023) 154187.
[18] D. Catalini, D. Kaoumi, A.P. Reynolds, G.J. Grant, Friction Consolidation of MA956 powder, Journal of Nuclear Materials 442(1-3) (2013) S112-S118.
[19] D. Zhang, J. Darsell, J. Wang, X. Ma, G. Grant, I. Anderson, J. Rieken, D. Edwards, W. Setyawan, T. Horn, No ball milling needed: Alternative ODS steel manufacturing with gas atomization reaction synthesis (GARS) and friction-based processing, Journal of Nuclear Materials 566 (2022) 153768.
[20] C. Huang, W. Li, Z. Zhang, M. Fu, M.-p. Planche, H. Liao, G. Montavon, Modification of a cold sprayed SiCp/Al5056 composite coating by friction stir processing, Surface and Coatings Technology 296 (2016) 69-75.
[21] C. Huang, W. Li, Y. Feng, Y. Xie, M.-P. Planche, H. Liao, G. Montavon, Microstructural evolution and mechanical properties enhancement of a cold-sprayed CuZn alloy coating with friction stir processing, Materials Characterization 125 (2017) 76-82.

[22] C. Huang, X. Yan, W. Li, W. Wang, C. Verdy, M. Planche, H. Liao, G. Montavon, Post-spray modification of cold-sprayed Ni-Ti coatings by high-temperature vacuum annealing and friction stir processing, Applied Surface Science 451 (2018) 56-66.

[23] K. Ross, B. Sutton, G. Grant, G. Cannell, G. Frederick, R. Couch, Development of Friction Stir Processing for Repair of Nuclear Dry Cask Storage System Canisters, in: Y. Hovanski, R. Mishra, Y. Sato, P. Upadhyay, D. Yan (Eds.) Friction Stir Welding and Processing IX, Springer International Publishing, Cham, 2017, pp. 39-46.

[24] T. Hidayat, D. Shishin, E. Jak, S.A. Decterov, Thermodynamic reevaluation of the Fe–O system, Calphad 48 (2015) 131-144.

[25] D. Zhang, J.T. Darsell, J. Wang, X. Ma, G.J. Grant, I.E. Anderson, J.R. Rieken, D.J. Edwards, W. Setyawan, T.J. Horn, G.R. Odette, No ball milling needed: Alternative ODS steel manufacturing with gas atomization reaction synthesis (GARS) and friction-based processing, Journal of Nuclear Materials 566 (2022) 153768.

[26] I.E. Anderson, R.L. Terpstra, Progress toward gas atomization processing with increased uniformity and control, Materials Science and Engineering: A 326(1) (2002) 101-109.

[27] J. Rieken, Gas atomized precursor alloy powder for oxide dispersion strengthened ferritic stainless steel, Ames Lab., Ames, IA (United States), 2011.

[28] X. Jiang, N. Overman, C. Smith, K. Ross, Microstructure, hardness and cavitation erosion resistance of different cold spray coatings on stainless steel 316 for hydropower applications, Materials Today Communications 25 (2020) 101305.

[29] X. Jiang, N. Overman, N. Canfield, K. Ross, Friction stir processing of dual certified 304/304L austenitic stainless steel for improved cavitation erosion resistance, Applied Surface Science 471 (2019) 387-393.

[30] B.H. Toby, R.B. Von Dreele, GSAS-II: the genesis of a modern open-source all purpose crystallography software package, Journal of Applied Crystallography 46(2) (2013) 544-549.

[31] K. Thompson, D. Lawrence, D.J. Larson, J.D. Olson, T.F. Kelly, B. Gorman, In situ site-specific specimen preparation for atom probe tomography, Ultramicroscopy 107(2) (2007) 131-139.

[32] T.S. Byun, B.E. Garrison, M.R. McAlister, X. Chen, M.N. Gussev, T.G. Lach, A.L. Coq, K. Linton, C.B. Joslin, J.K. Carver, F.A. List, R.R. Dehoff, K.A. Terrani, Mechanical behavior of additively manufactured and wrought 316L stainless steels before and after neutron irradiation, Journal of Nuclear Materials 548 (2021) 152849.

[33] A. international, E8/E8M-16a: Standard Test Methods for Tension Testing of Metallic Materials, ASTM international2016.

[34] R.L. Whitesell, I.E. Anderson, E.A. Rinko, E.M. White, T.E. Prost, T. Eden, T.A. Palmer, Results of experiments with cold spray deposition of Fe-based ODS alloys using as-atomized spherical GARS powder, 2019 International Conference on Powder Metallurgy and Particulate Materials, POWDERMET 2019, Metal Powder Industries Federation, 2020, pp. 486-499.

[35] R.S. Mishra, Z. Ma, Friction stir welding and processing, Materials science and engineering: R: reports 50(1-2) (2005) 1-78.

[36] A. Naskar, M. Bhattacharyya, K.S. Raja, I. Charit, J. Darsell, S. Jana, Pitting behavior of friction stir repair-welded 304L stainless steel in 3.5% NaCl solution at room temperature: role of grain and defect structures, SN Applied Sciences 2(12) (2020) 1-21.

[37] M.A. Auger, V. de Castro, T. Leguey, S. Lozano-Perez, P.A.J. Bagot, M.P. Moody, S.G. Roberts, Effect of the milling atmosphere on the microstructure and mechanical properties of a ODS Fe-14Cr model alloy, Materials Science and Engineering: A 671 (2016) 264-274.

[38] A. Etienne, N.J. Cunningham, Y. Wu, G.R. Odette, Effects of friction stir welding and post-weld annealing on nanostructured ferritic alloy, Materials Science and Technology 27(4) (2011) 724-728.

[39] M.E. Alam, S. Pal, K. Fields, S.A. Maloy, D.T. Hoelzer, G.R. Odette, Tensile deformation and fracture properties of a 14YWT nanostructured ferritic alloy, Materials Science and Engineering: A 675 (2016) 437-448.

[40] M.E. Alam, S. Pal, S.A. Maloy, G.R. Odette, On delamination toughening of a 14YWT nanostructured ferritic alloy, Acta Materialia 136 (2017) 61-73.
[41] J.H. Kim, T.S. Byun, D.T. Hoelzer, S.-W. Kim, B.H. Lee, Temperature dependence of strengthening mechanisms in the nanostructured ferritic alloy 14YWT: Part I—Mechanical and microstructural observations, Materials Science and Engineering: A 559 (2013) 101-110.
[42] VRC, Cold Spray vs Thermal Spray – An Overview, 2020. https://www.vrcmetalsystems.com/blog-post/cold-spray-vs-thermal-spray/. (Accessed 07/18/2020 2020).
[43] K.A. Ross, M. Alabi, Update on Investigations of Viability of Cold Spray and FSW as a Spent Nuclear Fuel Dry Storage Canister Mitigation Tool, Pacific Northwest National Lab.(PNNL), Richland, WA (United States), 2019.
[44] H. Jia, Z. Zhou, S. Li, A new strategy for additive manufacturing ODS steel using Y-containing gas atomized powder, Materials Characterization 187 (2022) 111876.
[45] S. Saptarshi, M. DeJong, C. Rock, I. Anderson, R. Napolitano, J. Forrester, S. Lapidus, D. Kaoumi, T. Horn, Laser Powder Bed Fusion of ODS 14YWT from Gas Atomization Reaction Synthesis Precursor Powders, JOM 74(9) (2022) 3303-3315.
[46] S. Takaki, Review on the Hall-Petch relation in ferritic steel, Materials Science Forum, Trans Tech Publ, 2010, pp. 11-16.
[47] R.Z. Valiev, R.K. Islamgaliev, I.V. Alexandrov, Bulk nanostructured materials from severe plastic deformation, Progress in materials science 45(2) (2000) 103-189.
[48] J.H. Kim, T.S. Byun, D.T. Hoelzer, C.H. Park, J.T. Yeom, J.K. Hong, Temperature dependence of strengthening mechanisms in the nanostructured ferritic alloy 14YWT: Part II—Mechanistic models and predictions, Materials Science and Engineering: A 559 (2013) 111-118.
[49] S. Ukai, 4.08 - Oxide Dispersion Strengthened Steels, in: R.J.M. Konings (Ed.), Comprehensive Nuclear Materials, Elsevier, Oxford, 2012, pp. 241-271.
[50] J.H. Schneibel, M. Heilmaier, Hall–Petch breakdown at elevated temperatures, Materials Transactions 55(1) (2014) 44-51.
[51] W. Xiaolei, J. Ping, C. Liu, Y. Fuping, Y.T. Zhu, Extraordinary strain hardening by gradient structure, Proceedings of the National Academy of Sciences of the United States of America 111(20) (2014) 7197-201.

Figure 1

Click here to access/download;Figure;Fig1.jpg

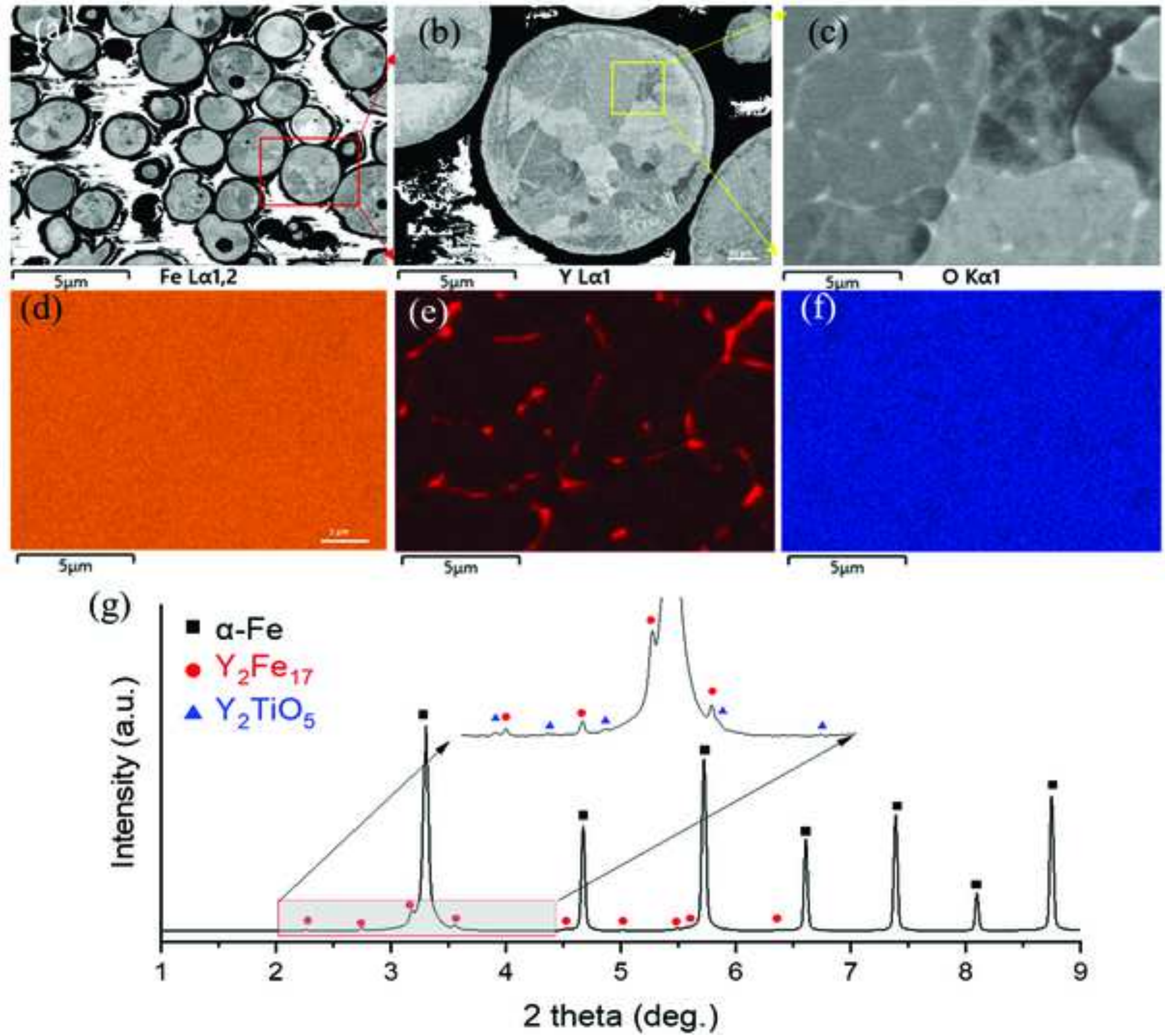

Figure 2

Click here to access/download;Figure;Fig2.jpg

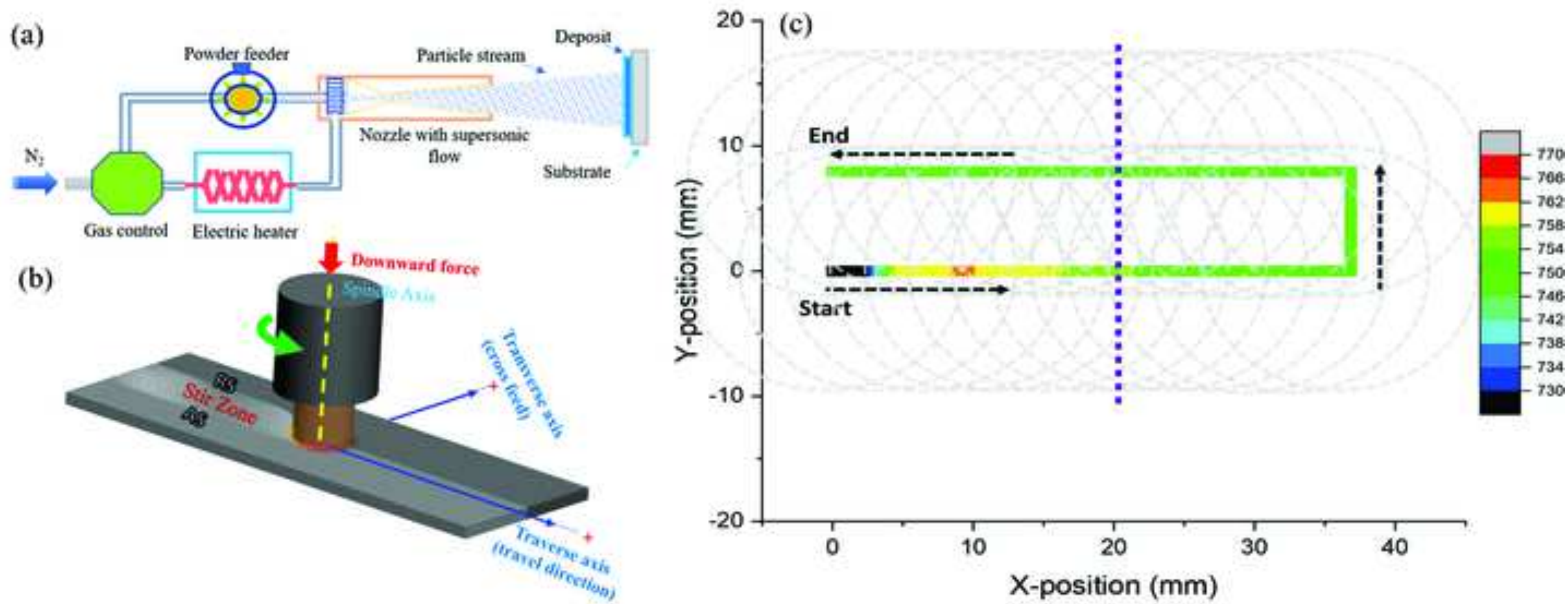

Figure 3

Click here to access/download;Figure;Fig3.jpg

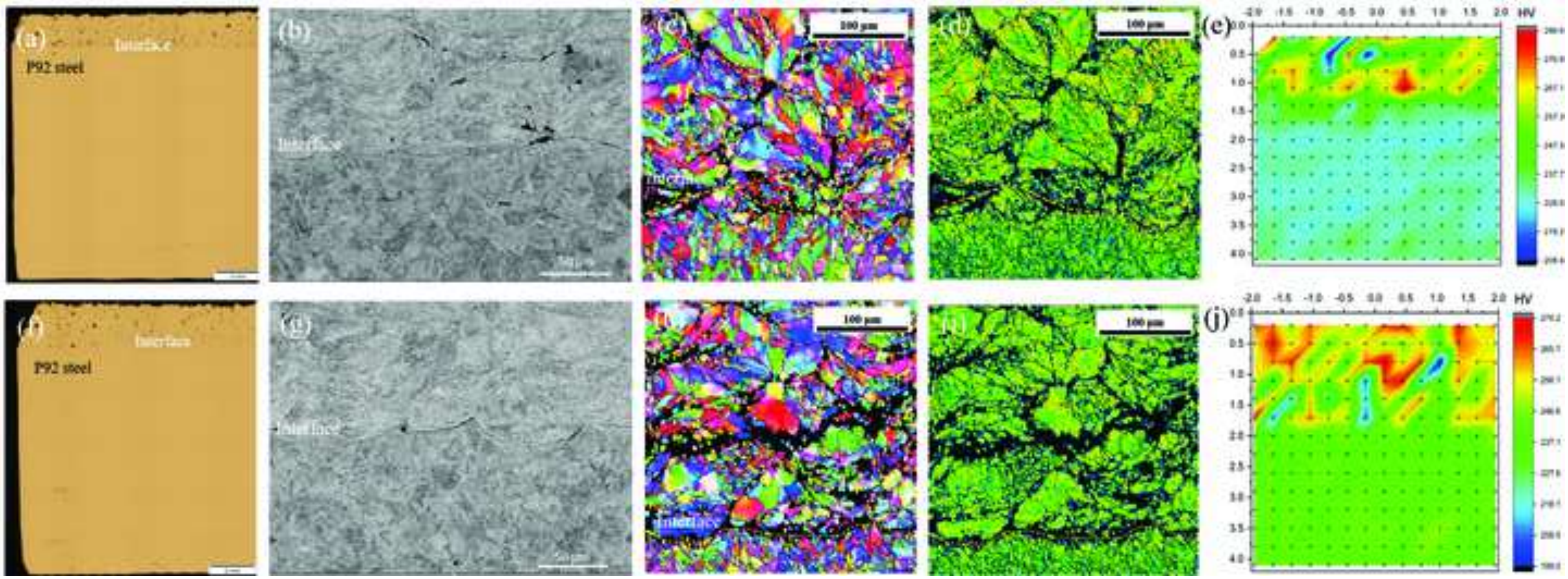

Figure 4

Click here to access/download;Figure;Fig4.jpg

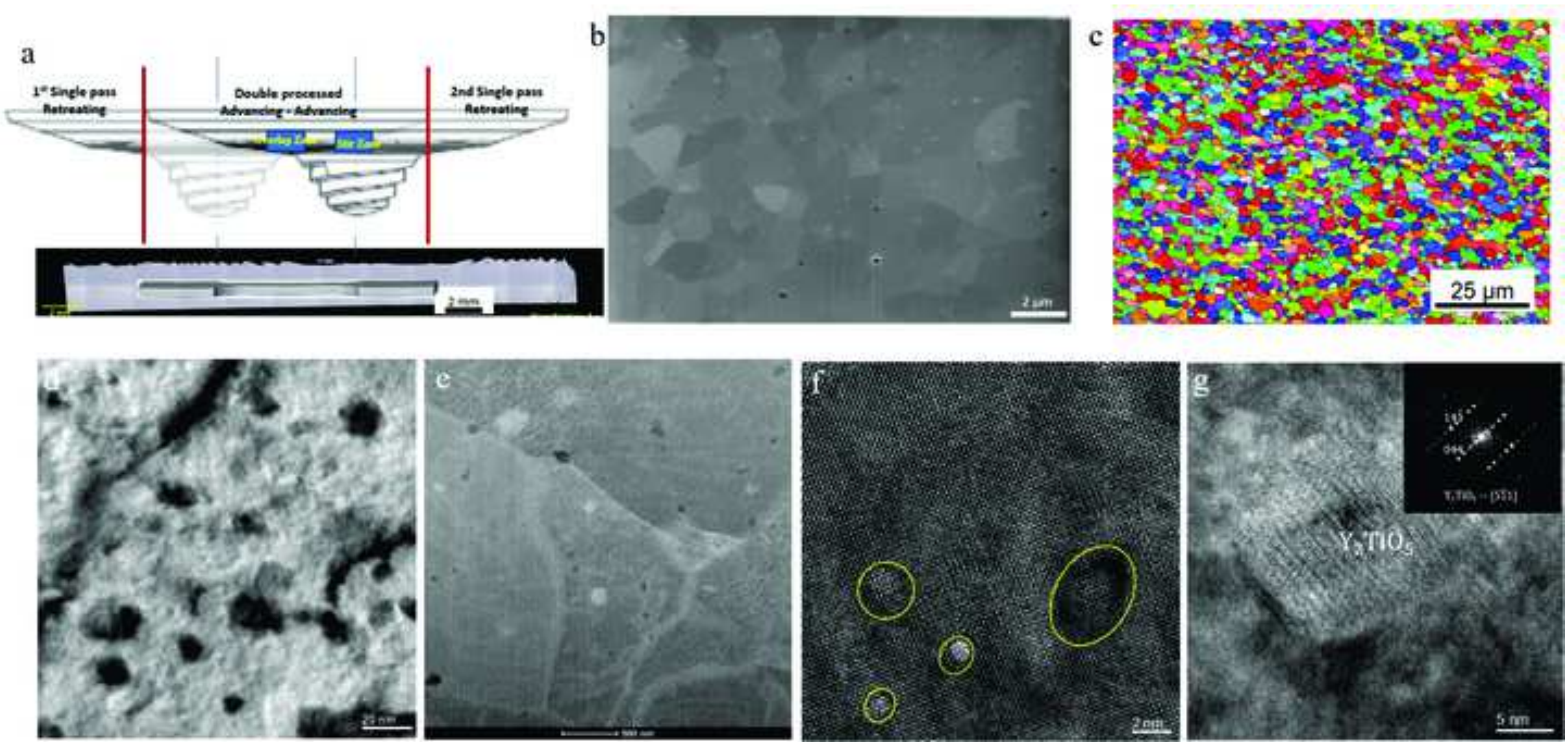

Figure 5

Click here to access/download;Figure;Fig5.jpg

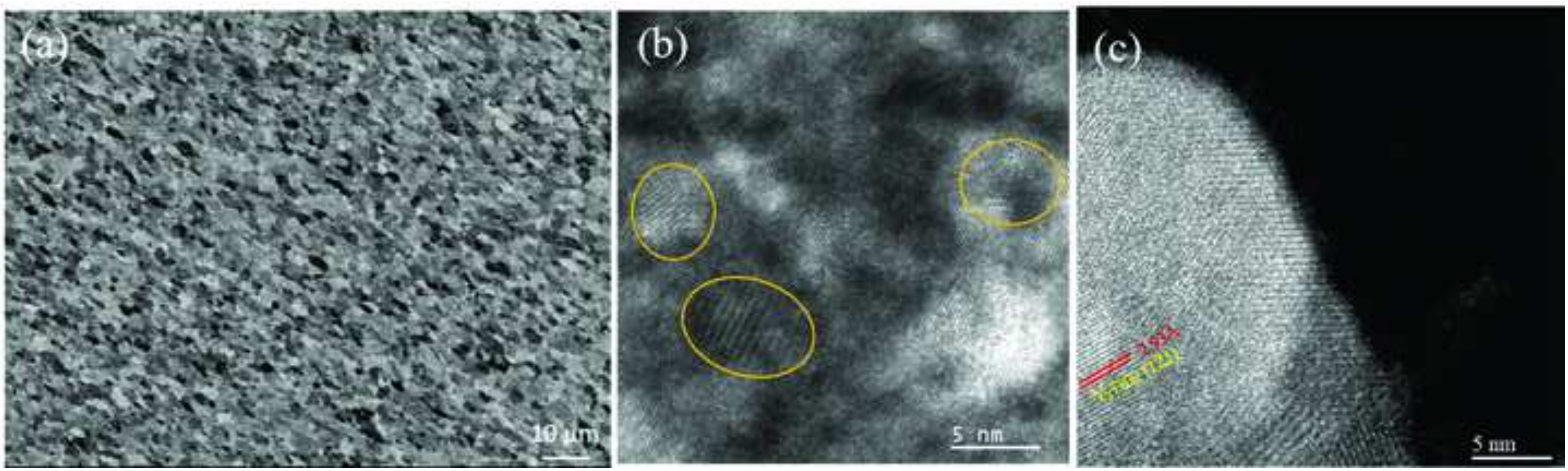

Figure 6

Click here to access/download;Figure;Fig6.jpg

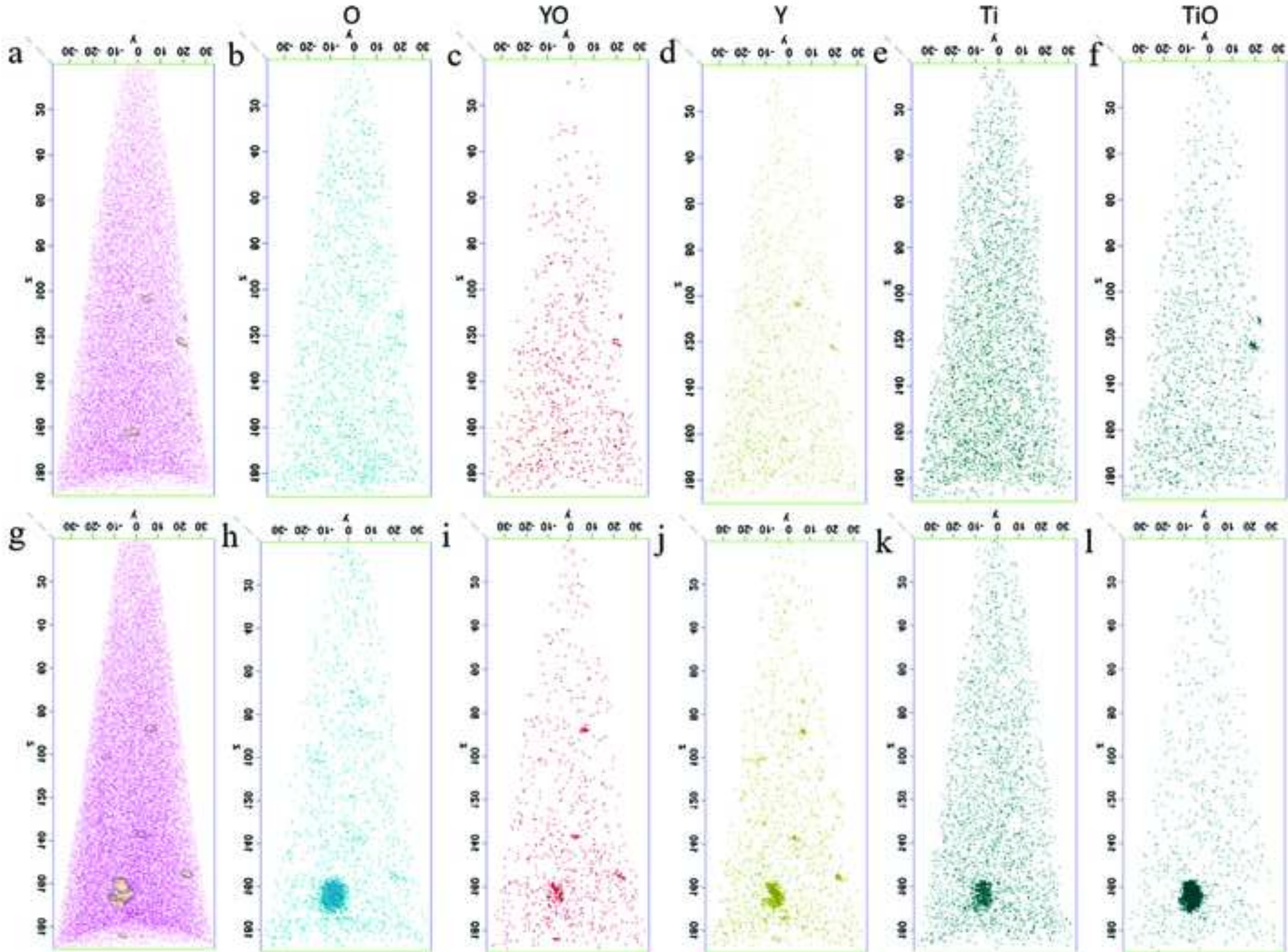

Figure 7

Click here to access/download;Figure;Fig7.jpg

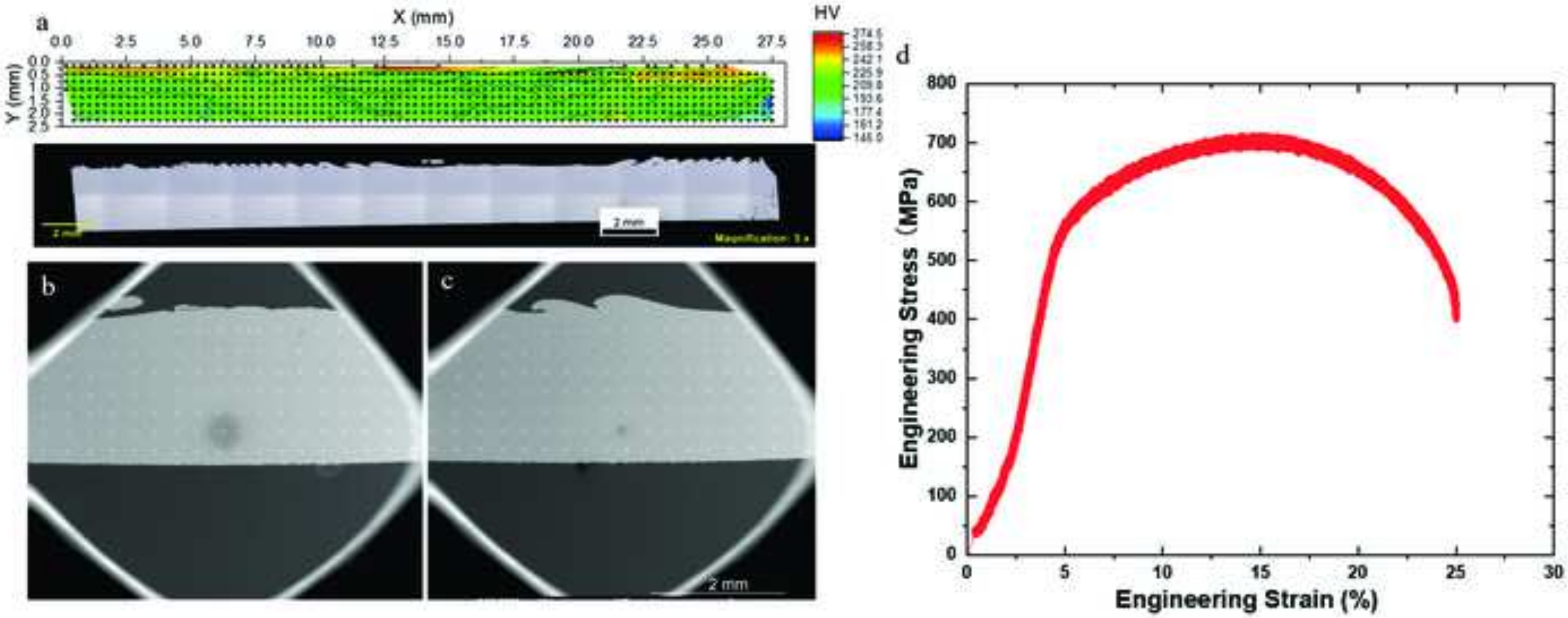

Xiang Wang: Validation, Formal analysis, Investigation, Writing - Original Draft, Writing - Review & Editing, Visualization. **Dalong Zhang**: Conceptualization, Methodology, Formal analysis, Investigation, Writing - Original Draft, Writing – Review & Editing, Visualization, Supervision, Funding acquisition. **Jens Darsell**: Methodology, Investigation, Writing - Review & Editing. **Kenneth Ross**: Methodology, Investigation, Writing - Review & Editing. **Xiaolong Ma**: Formal analysis, Visualization. **Jia Liu**: Formal analysis, Visualization. **Tingkun Liu**: Formal analysis, Visualization. **Ramprashad Prabhakaran**: Validation, Formal Analysis. **Lan Li**: Validation, Visualization. **Iver Anderson**: Resources, Writing - Review & Editing. **Wahyu Setyawan**: Resources, Supervision.

Declaration of interests

☒ The authors declare that they have no known competing financial interests or personal relationships that could have appeared to influence the work reported in this paper.

☐The authors declare the following financial interests/personal relationships which may be considered as potential competing interests: